

## An Improved Direct Adaptive Fuzzy Controller for an Uncertain DC Motor Speed Control System

Duc-Cuong Quach<sup>\*1</sup>, Shuang Huang<sup>2</sup>, Quan Yin<sup>3</sup>, Chunjie Zhou<sup>4</sup>

<sup>1,2,3,4</sup>Department of Control Science and Engineering, Huazhong University of Science and Technology, Wuhan, 430074, P.R. China

\*Corresponding author, e-mail e-mail: quachcuong304@gmail.com<sup>1</sup>, huangshuang@hust.edu.cn<sup>2</sup>, : yinquans@163.com<sup>3</sup>, cjiezhou@mail.hust.edu.cn<sup>4</sup>

### Abstract

*In this paper, we present an improved Direct Adaptive Fuzzy (IDAF) controller applied to general control DC motor speed system. In particular, an IDAF algorithm is designed to control an uncertain DC motor speed to track a given reference signal. In fact, the quality of the control system depends significantly on the amount of fuzzy rules-fuzzy sets and the updating coefficient of the adaptive rule. This can be observed clearly by the system error when the reference input is constant and out of a particular range or in the case of it varies with nonzero acceleration. So, in order to enhance quality of the system, increasing the amount of fuzzy sets and adjusting appropriately the updating coefficient of controller based on value of state error vector are needed. In addition, the proposed IDAF algorithm can control the DC motor speed under unstable supply voltages and varying loads. The control system is implemented on a dsPIC33FJ256MC710A 16-bit DSC (Digital Signal Processing Controller) board. Experimental results demonstrate the effectiveness of the proposed method.*

**Keywords:** DC motor, direct adaptive fuzzy controller, speed control, dsPIC

Copyright © 2013 Universitas Ahmad Dahlan. All rights reserved.

### 1. Introduction

Although inverter-induction motor drive systems have been developed very quickly in the field of electric drives, DC motor drives still play an important role in many industrial systems such as robotics, rolling mills, machine tools and especially in low power electrical drive systems [1-3]. In fact, the DC motor provides not only excellent control characteristics, but also large range of both supply voltage and power for many different applications. Traditionally, a PID controller or a control structure with two PI loops [14-17] is used in DC motor drive control systems. With simple structure and implementation, it works well if the model of DC motor is linear time-invariant [4]. However, most of the models of motors are non-linear time-variant at all operating points [15], for example, the old motors, or even the new ones under different conditions of load or/and different running environments, etc. These in turn make the PID and PI controllers challenging to achieve high control performance [14, 15]. To overcome this challenge, many control methods, e.g. PID-fuzzy, adaptive-fuzzy, neural-fuzzy, fuzzy-sliding mode, etc, have been proposed [2-5], [13-15].

Concerning with adaptive-fuzzy control, its main advantage is can deal with nonlinear uncertain systems. Many researchers have exploited this advantage to apply for a wide range of problems such as process control, motor drives, automotive, flight control, etc. However, there are still some open problems need to be investigated to improve the control quality of adaptive-fuzzy control method such as the number of fuzzy rules and the updating coefficient value of adaptive rule, etc [9]. In our work, we aim at designing and implementing a general controller using direct adaptive fuzzy to control a DC motor speed so as to track a reference signal with unknown parameters of DC motor, under varying loads and different supply voltage conditions. Furthermore, in order to improve the quality of the control systems, the number of fuzzy rules is increased and a G-Fuzzy system is used for online adjusting the updating coefficient (Figure 2). The IDAF consists of a fuzzy system and an adaptive control rule. It can on-line estimate the parameters of the fuzzy system to generate an optimal control law for controlling an uncertain nonlinear object [6-11]. The parameters of fuzzy system are updated by adaptive rule based on a Lyapunov approach. This control structure is shown in Figure 2 below.

To do so, the hardware is designed by dsPIC embedded system using dsPIC33FJ256MC710A chip, i.e. a 16-bit DSC with high speed, larger memory, and many powerful modules. More importantly, the dsPIC33FJ256MC710A is specially designed for motor control and power conversion [18]. The compiler for dsPIC is C language and MPLAB Integrated Development Environment.

The remainder of this paper is organized as follows. Section 2 describes the model of system and IDAF algorithm for DC control speed. Design and implementation system is shown in section 3. In section 4, we present experimental results and analysis. Finally, the conclusions are stated in section 5.

**2. Modeling of System and IDAF Algorithm for DC Motor Control Speed**

The detailed model of control object is shown in Figure 1. The input and output are the PWM value and the speed of DC motor, respectively. When the frequency of the H-bridge DC chopper is high enough, the DC voltage output of the chopper are commensurable with  $u$ . Where,  $u$  is control value, which depends on active time in a cycle time of PWM signal.

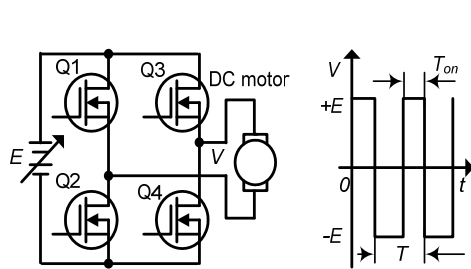


Figure 1. Control Object

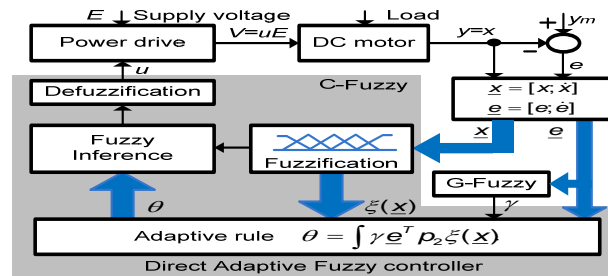


Figure 2. Control Structure

$$V = uE \tag{1}$$

The modeling of DC motor-H bridge DC chopper is described as below

$$\begin{cases} \ddot{x} = -\left(\frac{JR + LK_f}{JL}\right)\dot{x} - \left(\frac{RK_f + K_e K_t}{JL}\right)x + \frac{K_t E}{JL}u \\ y = x \end{cases} \tag{2}$$

where,  $y$  is the speed of motor.  $R, L, K_e$  and  $K_t$  are resistance, inductance, voltage constant and torque constant.  $K_f$  and  $J$  are dynamic friction constant and inertia respectively of system. The IDAF controller is designed to control the speed of a general DC motor system, therefore motor parameters such as  $R, L, K_e$ , etc are unknown.

In Figure 2 shows the controller structure in which the C-Fuzzy controller directly controls the plant and the G-Fuzzy controller adjusts the updating coefficient  $\gamma$  of the adaptive rule. From equation (2) we have the optimal control law as below

$$u^* = \frac{1}{b}(\ddot{x} - f(x)) \tag{3}$$

where, the state vector  $\underline{x} = [x, \dot{x}]^T$ ,  $b = (K_t E) / (JL) > 0$  and  $f(\underline{x}) = a_1 \dot{x} + a_2 x$  ( $a_1$  and  $a_2$  rely on motor parameters). In equation (3)  $f(\underline{x})$  and  $b$  are unknown, leading to the fact that  $u^*$  cannot be implemented. However, we can design a Takagi-Sugeno (T-S) fuzzy system in which the output  $\hat{u}(\underline{x} | \theta)$  is to approximate the optimal control law  $u^*$  [8-11].

The T-S fuzzy system consist of two inputs  $x, \dot{x}$ , one output  $\hat{u}(\underline{x} | \theta)$ , and it is described by a collection fuzzy rule as follows

If  $x$  is  $SP_i$  and  $\dot{x}$  is  $AC_j$  then  $u_{ij} = \theta_{ij}$

where,  $SP_i (1 \leq i \leq n)$  and  $AC_j (1 \leq j \leq m)$  are the fuzzy variables characterized by the membership functions  $\mu_i^x$  and  $\mu_j^{\dot{x}}$  of variables  $x$  and  $\dot{x}$ . When the product inference and the center of gravity defuzzification single method are used, the output of the T-S fuzzy system is

$$\hat{u}(\underline{x} | \theta) = \frac{\sum_{i=1}^n \sum_{j=1}^m \theta_{ij} \mu_i^x(x) \mu_j^{\dot{x}}(\dot{x})}{\sum_{i=1}^n \sum_{j=1}^m \mu_i^x(x) \mu_j^{\dot{x}}(\dot{x})} \quad (4)$$

$$\hat{u}(\underline{x} | \theta) = \theta \xi(\underline{x}) \quad (5)$$

Where,

$$\theta = \begin{bmatrix} \theta_{11} & \theta_{12} & \dots & \theta_{1m} \\ \theta_{21} & \theta_{22} & \dots & \theta_{2m} \\ \vdots & \vdots & \ddots & \vdots \\ \theta_{n1} & \theta_{n2} & \dots & \theta_{nm} \end{bmatrix}, \quad \xi(\underline{x}) = \begin{bmatrix} \xi_{11}(\underline{x}) & \xi_{12}(\underline{x}) & \dots & \xi_{1m}(\underline{x}) \\ \xi_{21}(\underline{x}) & \xi_{22}(\underline{x}) & \dots & \xi_{2m}(\underline{x}) \\ \vdots & \vdots & \ddots & \vdots \\ \xi_{n1}(\underline{x}) & \xi_{n2}(\underline{x}) & \dots & \xi_{nm}(\underline{x}) \end{bmatrix} \quad \text{and} \quad \xi_{ij}(\underline{x}) = \frac{\mu_i^x(x) \mu_j^{\dot{x}}(\dot{x})}{\sum_{i=1}^n \sum_{j=1}^m \mu_i^x(x) \mu_j^{\dot{x}}(\dot{x})}$$

Here,  $\theta$  is an adjustable parameter matrix and  $\xi(\underline{x})$  is a matrix of fuzzy basis function.  $\hat{u}(\underline{x} | \theta)$  can approach  $u^*$  and satisfy the Lyapunov stability criterion when  $\theta$  matrix is updated by equation (6), [7-10].

$$\dot{\theta} = \gamma \underline{e}^T p_2 \xi(\underline{x}) \quad (6)$$

where  $\gamma$  is a positive updating coefficient,  $\underline{e} = [e, \dot{e}]$  is an error vector and  $p_2$  is the last column of  $P_{2 \times 2}$  matrix,  $P$  is the root of the Lyapunov equation (7).

$$A^T P + P A = -Q \quad (7)$$

In the equation (7),  $Q$  is an arbitrary positive definite symmetric matrix and  $A$  is a state matrix of error. The matrix  $A$  based on exact differential equation of error  $\ddot{e} + k_1 \dot{e} + k_2 e = 0$ , so  $A = [0, 1; -k_2, -k_1]$ .

As mentioned above, the quality of control system depends significantly on the number of fuzzy rules and the updating coefficient  $\gamma$  of the adaptive rule. It is easy to see that, the more number of fuzzy rules is the more accuracy in approximating of the optimal control signal  $u^*$  becomes. However, if the number of fuzzy rules is too large, it will increase the processing time of the controller. Therefore, it is necessary to design an appropriate number of fuzzy rules for a particular system. Figure 5 describes a simple method to increase the number of fuzzy rules while still remain the processing time of controller small enough. In the term of the updating coefficient, equation (6) indicate that, when  $\gamma$  is large, the updated value of  $\theta$  is more sensitive to the error, so the effect of the updating law to the system is stronger.

However, when the error is small, if  $\gamma$  is still too large, the output response oscillates largely around the reference point. Therefore, it is necessary for us to adjust online appropriately the value of the updating coefficient using the G-Fuzzy controller. The next sections present the system implementation and describe clearly the benefit of our method based on experimental results.

### 3. Configuration and Implementation

#### 3.1. System Hardware Configuration

In this section, we used the dsPIC33FJ256MC710A chip to implement the algorithm. This is the latest version of motor control and power conversion 16-bit digital signal processing controller of Microchip with many powerful features for control motor.

In this system (Figure 3 and Figure 4), the clock speed of dsPIC is set to 40 (MHz) and the chip is supplied by a 3.3 (V) source. The TIMER1 interrupt is used to sample the data, sampling time is 5.0 (ms). In the PWM module, PWM1 is to control the H-bridge DC chopper and PWM2 is to change the load of DC generator. The PWM resolution is selected 12-bit data, therefore the switching frequency of the PWM signal is 9.775 (KHz). The interface between PC and dsPIC is UART1 and the baud rate is set to 19200 (bps).

Table 1. Devices of Hardware System

Device	Parameters
CPU	dsPIC33FJ256MC710A, 40MHz
DC machines	D06D03 30 (V), 2 (A), 3100 (rpm)
DC supply	30 (V), 5 (A)
Encoder	3000 (ppr)
Current sensor	CSNE151-100
Power drive	MOSFET H-bridge chopper



Figure 3. Experiment Hardware

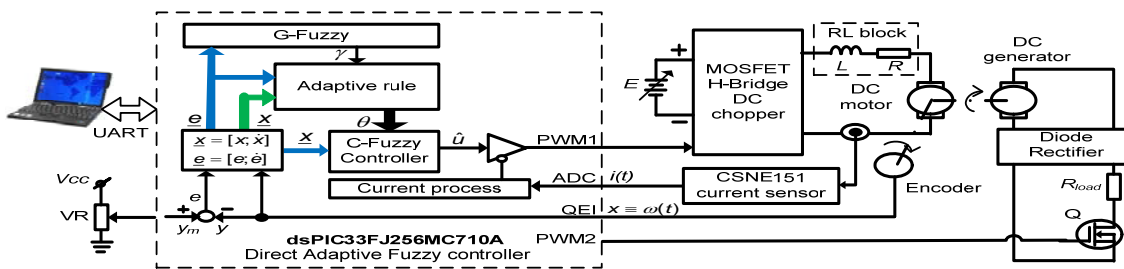


Figure 4. Hardware Block Diagram of Control System

The speed feedback loop uses a 3000 (ppr) encoder. The QEI module in dsPIC is set to operate at x4 mode, with 5.0 (ms) sampling time such that the speed  $y = n_e$  ( $n_e$  is the number of pulses reading from POS1CNT register of QEI module per each sample). The current sensor is Honeywell CSNE151-100, its maximum value is set to 6 (A), the signal of this sensor is connected to the ADC0 channel for short circuit and overload protection. In order to view the supply voltage  $E$  in some experimental cases, we use the HCNR200 high-linearity analog optocoupler and the ADC1 channel. The ADC module is setup in 12-bit resolution mode.

IRF460 MOSFET is used to design the H-bridge DC chopper. The power circuit is insulated from the control circuit by TLP250 optocouplers and the dead time of MOSFETs is set to 1.0 ( $\mu$ s). The voltage supply of chopper is subjected to be changed in the range from 0 to 30 (V). The motor and generator are all from D06D03 DC machine of Hitachi.

#### 3.2. Implementation DAF Controller

The IDAF controller is designed to control the DC motor speed in the range from -3000 to 3000 (rpm). The IDAF algorithm in dsPIC embedded system is described in sequel.

The T-S fuzzy system is used to design the controller. This fuzzy system includes two inputs of speed, acceleration and one output. The output value of fuzzy system is the control signal, i.e. PWM value. The speed is  $x$ ,  $x \in [-3200, 3200]$  (rpm), it is fuzzified using  $SP_i$  fuzzy sets with  $i = 1 \div 7$  and the membership functions are normalized  $[0, 320]$ . The acceleration variable is  $\dot{x}$ . In fact, the step response of some DC motors can be stable after 0.05 (s) with amplitude 3000 (rpm) so that  $\dot{x}$  can be set in the range of  $[-60000, 60000]$ (rpm/s). It is fuzzified

using  $AC_j$  fuzzy sets with  $j = 1 \div 7$  and the membership functions are normalized  $[0, 300]$ , all is shown in Figure 5. The output  $\hat{u}(x | \theta)$  of fuzzy system,  $\hat{u}(x | \theta) \in [-2048, 2047]$  is referred to  $V$  value of the supply from  $[-E, +E]$  so that the value of P1DC1 register (PWM module) is in the range  $[0, 4095]$ . The membership function of  $\hat{u}(x | \theta)$  is singleton fuzzy sets  $\theta_{ij}$ .

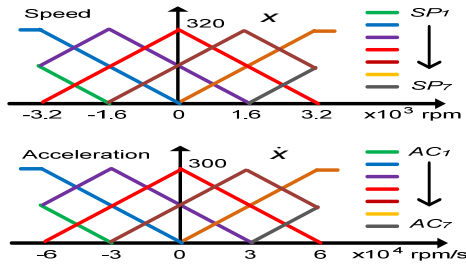


Figure 5. Fuzzy Sets of Speed and Acceleration Variables

Table 2. Tabular Structure of a Numerical Fuzzy Rules Base

$x \setminus \dot{x}$	$AC_1$	$AC_2$	$AC_3$	$AC_4$	$AC_5$	$AC_6$	$AC_7$
$SP_1$	$\theta_{11}$	$\theta_{12}$	$\theta_{13}$	$\theta_{14}$	$\theta_{15}$	$\theta_{16}$	$\theta_{17}$
$SP_2$	$\theta_{21}$	$\theta_{22}$	$\theta_{23}$	$\theta_{24}$	$\theta_{25}$	$\theta_{26}$	$\theta_{27}$
$SP_3$	$\theta_{31}$	$\theta_{32}$	$\theta_{33}$	$\theta_{34}$	$\theta_{35}$	$\theta_{36}$	$\theta_{37}$
$SP_4$	$\theta_{41}$	$\theta_{42}$	$\theta_{43}$	$\theta_{44}$	$\theta_{45}$	$\theta_{46}$	$\theta_{47}$
$SP_5$	$\theta_{51}$	$\theta_{52}$	$\theta_{53}$	$\theta_{54}$	$\theta_{55}$	$\theta_{56}$	$\theta_{57}$
$SP_6$	$\theta_{61}$	$\theta_{62}$	$\theta_{63}$	$\theta_{64}$	$\theta_{65}$	$\theta_{66}$	$\theta_{67}$
$SP_7$	$\theta_{71}$	$\theta_{72}$	$\theta_{73}$	$\theta_{74}$	$\theta_{75}$	$\theta_{76}$	$\theta_{77}$

The fuzzy logic controller has 49 fuzzy rules, they are shown in Table 2. In this paper, we apply the defuzzification method given by

$$\hat{u}(x(k) | \theta(k)) = \frac{\sum_{i=1}^7 \sum_{j=1}^7 \theta_{ij} \mu_i^x(x(k)) \mu_j^{\dot{x}}(\dot{x}(k))}{\sum_{i=1}^7 \sum_{j=1}^7 \mu_i^x(x(k)) \mu_j^{\dot{x}}(\dot{x}(k))} \tag{8}$$

The task of adaptive rule is to update the  $\theta_{ij}$  parameter in formula(8). The discrete equation of (8) can be written by

$$\begin{cases} \Delta \theta_{ij}(k) = \gamma \underline{e}(k)^T \underline{p}_2 \xi(x(k), \dot{x}(k)) \\ \theta_{ij}(k+1) = \theta_{ij}(k) + \Delta \theta_{ij}(k) \end{cases} \tag{9}$$

Selecting  $k_1 = 10$ ,  $k_2 = 50$ ,  $Q=[100, 0; 0, 100]$ , resulting in  $P= [265, 1; 1, 5.1]$ , and thus  $\underline{p}_2=[1; 5.1]$ .

Table 3. Fuzzy Sets of G-Fuzzy Controller

Variable	Fuzzy sets	Value	Normalized
$e$	PB, PS, ZZ, NS, NB	$-100 \div 100$	$-100 \div 100$
$\dot{e}$	PB, PS, ZZ, NS, NB	$-10000 \div 10000$	$-50 \div 50$
$\gamma$	VB, B, M, S, VS	$1 \div 5$	$10 \div 50$

Table 4. Fuzzy Rules of G-Fuzzy Controller

$e \setminus \dot{e}$	NB	NS	ZZ	PS	PB
NB	VB	VB	M	M	M
NS	VB	B	M	S	VS
ZZ	VS	S	S	S	VS
PS	VS	S	M	B	VB
PB	M	M	M	VB	VB

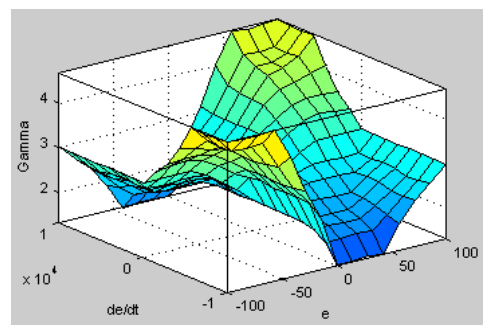


Figure 6. G-Fuzzy Surface

The period of calculating the updating coefficient  $\gamma$  is larger five times than the sampling time of the C-Fuzzy controller. The G-Fuzzy controller uses Mamdani fuzzy inference depicted

in Table 4 and center of gravity defuzzification method to adjust the output  $\gamma$  based on two input signals that are  $x$  and  $\dot{x}$ . The controller fuzzy sets are triangular form as shown in Table 3. Surface characteristic of G-Fuzzy controller and algorithm of control system are shown in Figure 6 and Figure 7.

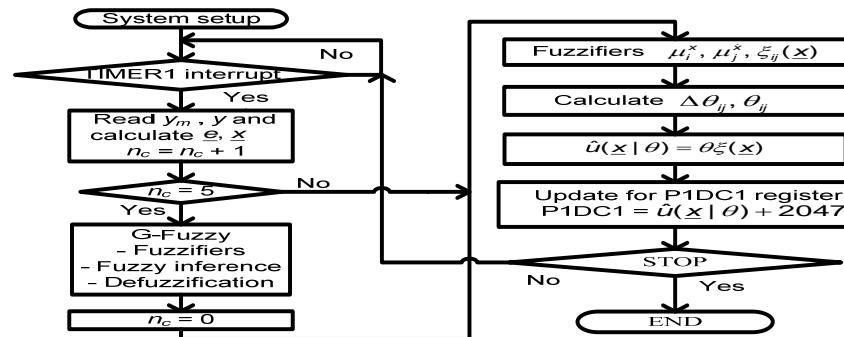


Figure 7. Algorithm of System

#### 4. Experimental Results and Analysis

The hardware system-based IDAF controller for the DC motor speed control system, which is developed and tested in this paper (shown in Figure 3 and Figure 4). During the process of testing, the reference speed  $y_m(k)$  is sent to the dsPIC from PC, all data of the system such as control signal  $\hat{u}(k)$ , real motor speed  $y(k)$ , current  $i(k)$  of DC motor and voltage  $E(k)$  of supply are saved to the RAM of dsPIC. When the testing finishes, these data are sent back to PC. The experimental results are obtained from five particular cases as follows.

The first case: We analysis the system error corresponds to three particular situation of  $\gamma$  that are  $\gamma$  is a large constant ( $\gamma = 5.0$ ),  $\gamma$  is a small constant ( $\gamma = 1$ ) and  $\gamma$  varies under adjusting of the G-Fuzzy controller. Let us first consider the situation that the reference speed varies with high acceleration as shown in Figure 8 (the periods are 0.0s - 1.2s, 2.4s - 4.2s and 5.5s - 8.5s). In such situation, when  $\gamma$  is small, the updating parameters  $\theta_{ij}$  of C-Fuzzy controller is updated with a small variation (i.e.,  $\Delta\theta_{ij}$  is small). That mean, the response ability of the C-Fuzzy controller is slow and this leads to the large system error. It is easy to observe from Figure 8 that the speed error for  $\gamma = 1.0$  (the black line) is very larger than the speed error for  $\gamma = 5.0$  (the red line) in this situation. Next, we consider the second situation that the reference speed is relatively stable (the periods are 1.2s - 2.4s, 4.2s - 5.5s and 8.5s - 10s). For this situation, when  $\gamma$  is large, the updating parameters  $\theta_{ij}$  of C-Fuzzy controller is updated with a large variation (i.e.,  $\Delta\theta_{ij}$  is large). That mean, the response ability of the C-Fuzzy controller is strong and this leads to the large oscillation of the motor speed around the reference point. The experimental results indicate in Figure 8 that the system error oscillates largely around the zero point in the case of  $\gamma = 5.0$ . From above two situations, it is worth mentioning that the control quality is significantly affected by the value of the updating coefficient  $\gamma$ . When the updating coefficient value is large, the response error reduces quickly. However, if the response error is small and the updating coefficient is still large, the response error then oscillates largely around the zero point. Therefore, it is necessary to adjust online the updating coefficient under the observation the response error to improve the system control quality. Figure 9 and Table 5 illustrate the rules of adjusting online the updating coefficient (This control strategy is present in Table 3, Table 4 and Figure 6 of the designing G-Fuzzy part). As shown in Figure 8, the final situation in which  $\gamma$  is adjusted online using our method, the speed error (blue line) is better than the both mentioned situations especially in the case of varying reference input. This also can be checked by ITAE-norm of the system error as presented in Table 6.

The second case: speed of DC motor tracks an output of reference model  $G(s)$  (transfer function  $G(s) = 1076 / (s^2 + 40s + 1076)$ ) under different  $R, L$  values. In the second case, the DC motor runs at 1200 (rpm) and rated current. The speed of DC motor tracks a reference speed which is the output of reference model. The time responses of system are shown in Figure 10

and Figure 11. In our testing, the model of DC motor is changed by RL block with  $R=2 (\Omega)$  and  $L=3(\text{mH})$ .

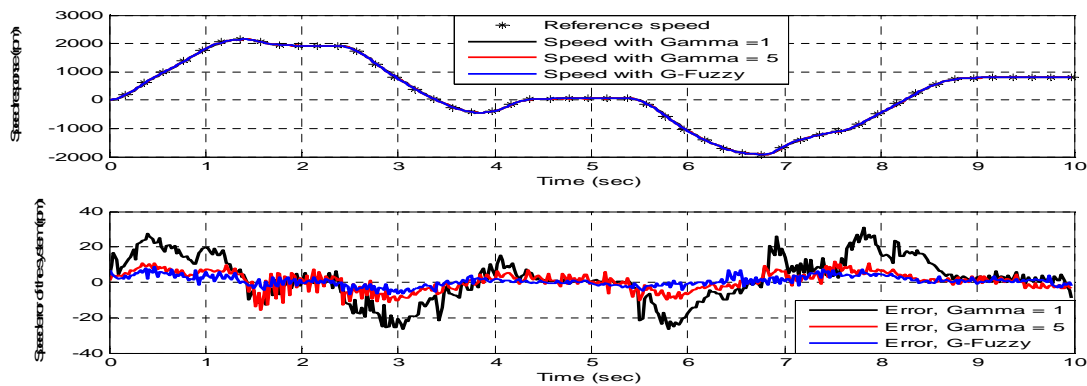


Figure 8. Speed and Error Responses in the First Case

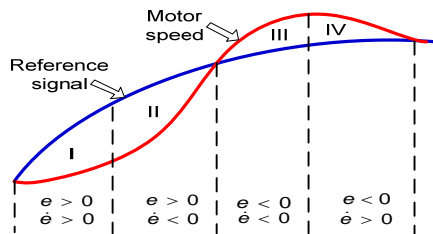


Table 5. Fuzzy Sets of G-Fuzzy Controller

Error area	Sign of error vector	$e^T p_2$	$\gamma$ value
I	$e > 0, \dot{e} > 0$	Positive	Big
II	$e > 0, \dot{e} < 0$	Positive	Mean
III	$e < 0, \dot{e} < 0$	Negative	Big
IV	$e < 0, \dot{e} > 0$	Negative	Mean

Figure 9. Analysis of  $\gamma$  in Error Areas

Table 6. ITAE-norm of System Error with Different  $\gamma$  Updating Coefficient Value

$\gamma$ coefficient	ITAE-norm	Time
1	425	10 (sec)
5	178	10 (sec)
G-Fuzzy	100	10 (sec)

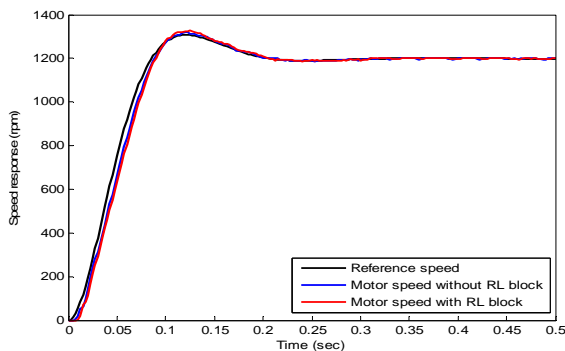


Figure 10. Speed Response of System in the Second Case

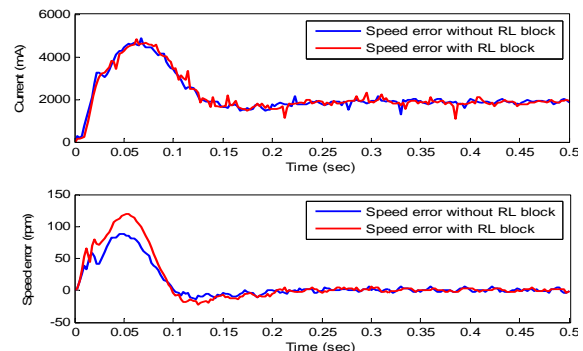


Figure 11. Current and Speed Error Response in the Second Case

The third case: The DC motor runs under varying load, different supply voltage condition, and the reference speed is step function. The results are shown in Figure 12 and Figure 13.

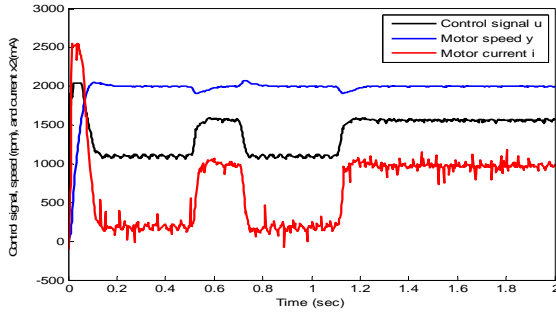


Figure 12. System Response under Variable Load in the Third Case

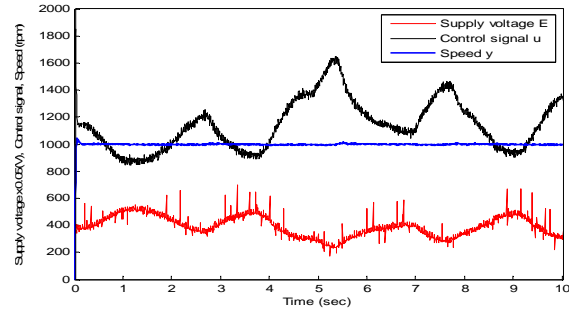


Figure 13. System Response under Variable Supply Voltage in the Third Case

The fourth case: The speed signal of motor tracks the reference speed signals in the form of step function as illustrated in Figure 14. The PWM value of control load circuit is constant so that the average current of DC motor only relies on the speed value of DC motor. The steady state errors and average current in this case are given in Table 7.

The fifth case: The speed tracks variable reference speed under varying load (Figure 15) (the PWM value of DC generator load is constant, leading to the result that the load of DC motor depends on the speed of motor, as shown in Figure 16). The result in Figure 16 also shows us the error in this case.

Table 7. Speed Error at Different Speed Value

Speed (rpm)	Current (mA)	Absolute error (rpm)	Relative error
-2000	-1600	±4	0.20%
-1500	-1150	±3	0.20%
-1000	-800	±4	0.40%
-500	-400	±2	0.40%
500	400	±2	0.40%
1000	800	±4	0.40%
1500	1150	±3	0.20%
2000	1600	±4	0.20%
2500	2040	±5	0.20%

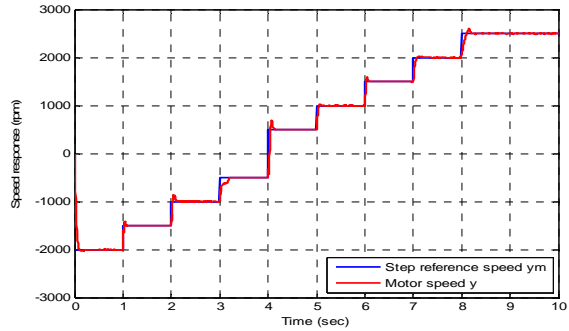


Figure 14. System Response in the Fourth Case

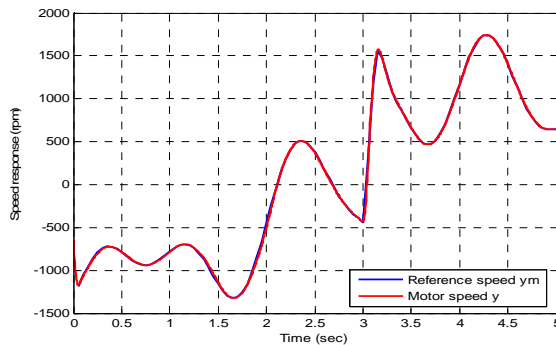


Figure 15. System Response in the Fifth Case

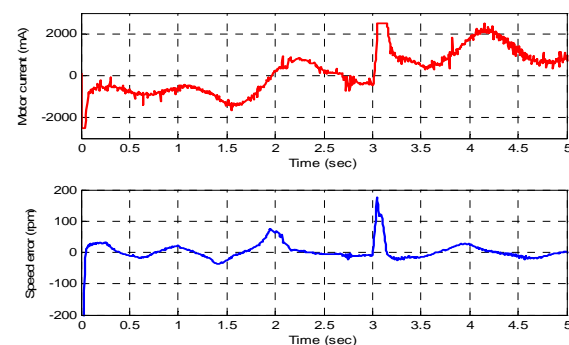


Figure 16. Motor Current and Steady Error in the Fifth Case

From Figure 10, it is clear to observe that when the resistance and inductance parameters of DC motor are changed, the speed response keeps invariant. When running the DC motor at 2000 (rpm), with speed reference in the form of step function, without load, the rise

time is 0.08 (s), and the overshoot is 2.5% (Figure 12). Figure 12 further describes the speed response when the step function of sudden loads appears, the DC motor runs from without load to with nominal load and vice versa. Under this varying load, the motor speed changes  $\pm 75$  (rpm) and the system becomes steady state in 0.09 (s). In fact, this changing value of speed depends on some conditions and parameters such as the updating coefficient  $\gamma$  of IDAF controller, the present speed value, the load and the system inertia  $J$ .

The tracking level between the motor speed and the reference speed is described in the fourth and fifth the cases. The reference speed is step function (Figure 14) or analog signal (Figure 15) with limit frequency and amplitude. Although load changes, the response speed of DC motor can tracks the reference speed value.

When reference speed is step function, the steady state error is shown in Table 7. In this table, we can see that the relative error of system depends on the present speed value of DC motor. At 500 (rpm) and 2500 (rpm) of the present speed, the relative errors are 0.40% and 0.20%, respectively. The experimental results show that steady state error is always different zero due to some reasons such as limit number of fuzzy rule-fuzzy set, relationship between encoder resolution and sampling time value, limit resolution and normalizing of calculation in the discrete system, etc.

## 5. Conclusion

In this paper, the design and implementation of an improved DAF controller based on a Lyapunov approach for control DC motor speed system is described. To improve the quality of control system, we mainly concentrate on develop the G-Fuzzy controller to adjust online the updating coefficient of the adaptive rule in the DAF controller. From the experimental results using dsPIC33FJ256MC710A chip, we observe that this controller is very suitable for high accuracy controlling a DC motor speed in case of: unknown modeling DC Motor, different supply voltage, and varying load. Furthermore, with this controller, it is very flexible to be applied, because if we know the order of object, we can design a control algorithm.

In our future work, the parameters of IDAF controller will be optimized to enhance the ability of IDAF controller. We further integrate a current controller into the system to control high power DC motors.

## References

- [1] AB Yildiz. Electrical equivalent circuit based modeling and analysis of direct current motors. *International Journal of Electrical Power & Energy Systems*. 2012; 43(1): 1043-1047.
- [2] GG Rigator. Adaptive fuzzy control of DC motors using state and output feedback. *Electric Power Systems Research Elsevier journal*. 2009; 79(11): 1579-1592.
- [3] AM Harb, IA Smadi. Tracking control of DC motors via mimo nonlinear fuzzy control. *Chaos, Solitons and Fractals Elsevier journal*. 2009; 42(2): 702-710.
- [4] DD Kukolj, SB Kuzmanovic, E Levi. Design of a PID-like compound fuzzy logic controller. *Engineering Applications of Artificial Intelligence*. 2001; 14(6): 785-803.
- [5] J Mendes, R Araujo, P Sousa, F Apostolo, L Alves. An architecture for adaptive fuzzy control in industrial environments. *Computer in Industry Journal*. 2011; 62(3): 364-373.
- [6] MA Khanesar, O Kaynak, M Teshnehlab. Direct Model Reference Takagi-Sugeno Fuzzy Control of SISO Nonlinear System. *IEEE Transactions on fuzzy systems*. 2011; 19(5): 914-924.
- [7] DL Tsay, HY Chung, CJ Lee. The adaptive control of nonlinear systems using the Sugeno-type of fuzzy logic. *IEEE Transactions on fuzzy systems*. 1999; 7(2): 225-129.
- [8] AE Ougli, I Iagrat, I Boumhidi. Direct Adaptive Fuzzy Control of Nonlinear Systems. *ICGST-ACSE Journal*. 2008; 8(2): 15-21.
- [9] LX Wang. Stable adaptive fuzzy control of nonlinear systems. *IEEE Transactions on fuzzy systems*. 1993; 1(2): 146-155.
- [10] M Bahita, K Belarbi. Feedback Adaptive control of a class of nonlinear systems using fuzzy approximators. *International Journal of Information Technology Convergence and Services*. 2011; 1(1): 14-29.
- [11] D Bellomo, D Naso, R Babuska. Adaptive fuzzy control of a non-linear servo-drive Theory and experimental results. *Engineering Applications of Artificial Intelligence*. 2008; 21(6): 846-857.

- 
- [12] AAA Emhemed, RB Mamat. *Modelling and Simulation for Industrial DC Motor Using Intelligent Control*. International Symposium on Robotics and Intelligent Sensors. Sarawak. 2012; 41: 420-425.
- [13] ML Hung, HT Yau, PY Chen, YH Su. *Intelligent Control Design and Implementation of DC Servo Motor*. International Symposium on Computer, Communication, Control and Automation. Tainan. 2010; 2: 369-372.
- [14] Yousif I, A Mashhadany. *Modeling and simulation of Adaptive Neuro-Fuzzy controller for Chopper-Fed DC Motor Drive*, IEEE Applied Power Electronics Colloquium. Johor Bharu. 2011; 110-115.
- [15] YL Cui, HL Lu, JB Fan. *Design and simulation of cascade fuzzy self-adaptive PID speed control of a thyristor-driven DC motor*. Proceeding of the Fifth International Conference on Machine Learning and Cybernetics. Dalian. 2006; 655-660.
- [16] R Garrido, D Calderon, A Soria. *Adaptive fuzzy control of DC motors*. IEEE International Power Electronics Congress. Puebla. 2006; 1-6.
- [17] HSh Xu, King, K King, Y Jani. *High Performance DC Chopper Speed and Current Control of Universal Motors Using a Microcontroller*. IEEE Industry Applications Conference 42nd IAS Annual Meeting. New Orleans, Louisiana. 2007; 701-705.
- [18] Microchip Technology Inc, dsPIC33FJXXXMCX06A/X08A/X10A Data Sheet. USA. 2011; 1-362.